



Potential risk to human skin cells from exposure to dicloran photodegradation products in water

Wei Xu^{a,*}, Emily N. Vebrosky^b, Kevin L. Armbrust^b

^a Department of Life Sciences, College of Science and Engineering, Texas A&M University Corpus Christi, Corpus Christi, Texas, USA

^b Department of Environmental Sciences, College of the Coast & Environment, Louisiana State University, Baton Rouge, Louisiana, USA



ARTICLE INFO

Handling Editor: Y.-G. Zhu

Keywords:

Docloran
Human skin
Phototoxicity
Inflammatory skin diseases

ABSTRACT

Exposure to sunlight and certain pesticides can induce phototoxic responses. Long- and short-term exposure to the photoactivated pesticides can cause a variety of skin diseases. However, assessment of pesticide phototoxicity on human skin is difficult. In the present study, human skin keratinocytes were cultured in several forms: monolayer cell sheet, three-dimensional culture, and keratinocyte-fibroblast co-culture. A common fungicide, dicloran (DC, 2,6-dichloro-4-nitroaniline), was irradiated with simulated sunlight for 2 (DC-PD-2h) and 4 (DC-PD-4h) hours. Dicloran, and two purified intermediate photodegradation products, 2-chloro-1,4-benzoquinone (CBQ) and 1,4-benzoquinone (BQ), were applied in toxicity tests independently with the keratinocyte culture models. The cell migration, cell differentiation, pro-inflammatory molecule production, and dermal fibroblast cell activation were all measured in the keratinocytes treated with the chemicals described above. These parameters were used as references for dicloran phototoxicity assessment. Among all tested chemicals, the DC-PD-4h and BQ demonstrated elevated toxicities to the keratinocytes compared to dicloran based on our results. The application of DC-PD-4h or BQ significantly delayed the migration of keratinocytes in monolayer cell sheets, inhibited the keratinocyte differentiation, increased the production of pro-inflammatory molecules by 3D keratinocyte culture, and enhanced the ability of 3D cultured keratinocytes in the activation of co-cultured dermal fibroblast cells. In contrast, dicloran, DC-PD-2h, and CBQ showed minimal effects on the keratinocytes in all assays. The results suggested that the four-hour photodegraded dicloran was likely to induce inflammatory skin diseases in the natural human skin. The 1,4-benzoquinone, which is the predominant degradation product detected following 4 h of irradiation, was the main factor for this response. Photoactivation increased the risk of skin exposed to dicloran in nature. Our models provided an efficient tool in the assessment of toxicity changes in pesticide following normal use practices under typical environmental conditions.

1. Introduction

Application of pesticides in agricultural production generates a large number of chemical wastes, which are released into the environment. Direct or indirect contact with these agrochemicals may affect human health depending on the type of pesticide. The United States Environmental Protection Agency (USEPA) has strictly regulated the usage and release of pesticides. However, assessing the toxicity of pesticides under specific conditions unique to particular chemical use patterns may not be addressed by the battery of regulatory studies required by the EPA in support of a pesticide's registration.

The environmental effects triggering modifications of the chemical structure of a pesticide to create more hazardous chemicals are an additional unknown risk factor.

Modification of compounds by environmental stresses has been identified in a number of recent studies. For example, the increase of environmental H⁺ leads to a reduced binding surface for positively charged metals, as most organic particles are negatively charged. Consequently, the organic complexes primarily formed by organic matter in seawater are reduced (Miller and Wootley, 2009), changing the bioavailability of organic contaminant compounds and other particulates. Additionally, the salinity change of the aquatic environment can alter the degradation and partitioning behavior of a chemical, contributing to chemical toxicity. A recent investigation suggested that the toxicity of the fungicide chlorothalonil to the estuarine grass shrimp, *Palaemonetes pugio*, was significantly elevated with a 10 ppt increase in salinity (DeLorenzo et al., 2009).

Another environmental factor that has demonstrated significant

* Corresponding author at: 6300 Ocean Dr. Corpus Christi, TX 78412.

E-mail address: wei.xu@tamucc.edu (W. Xu).

<https://doi.org/10.1016/j.envint.2018.10.010>

Received 22 June 2018; Received in revised form 4 October 2018; Accepted 6 October 2018

Available online 18 October 2018

0160-4120/ © 2018 Published by Elsevier Ltd.

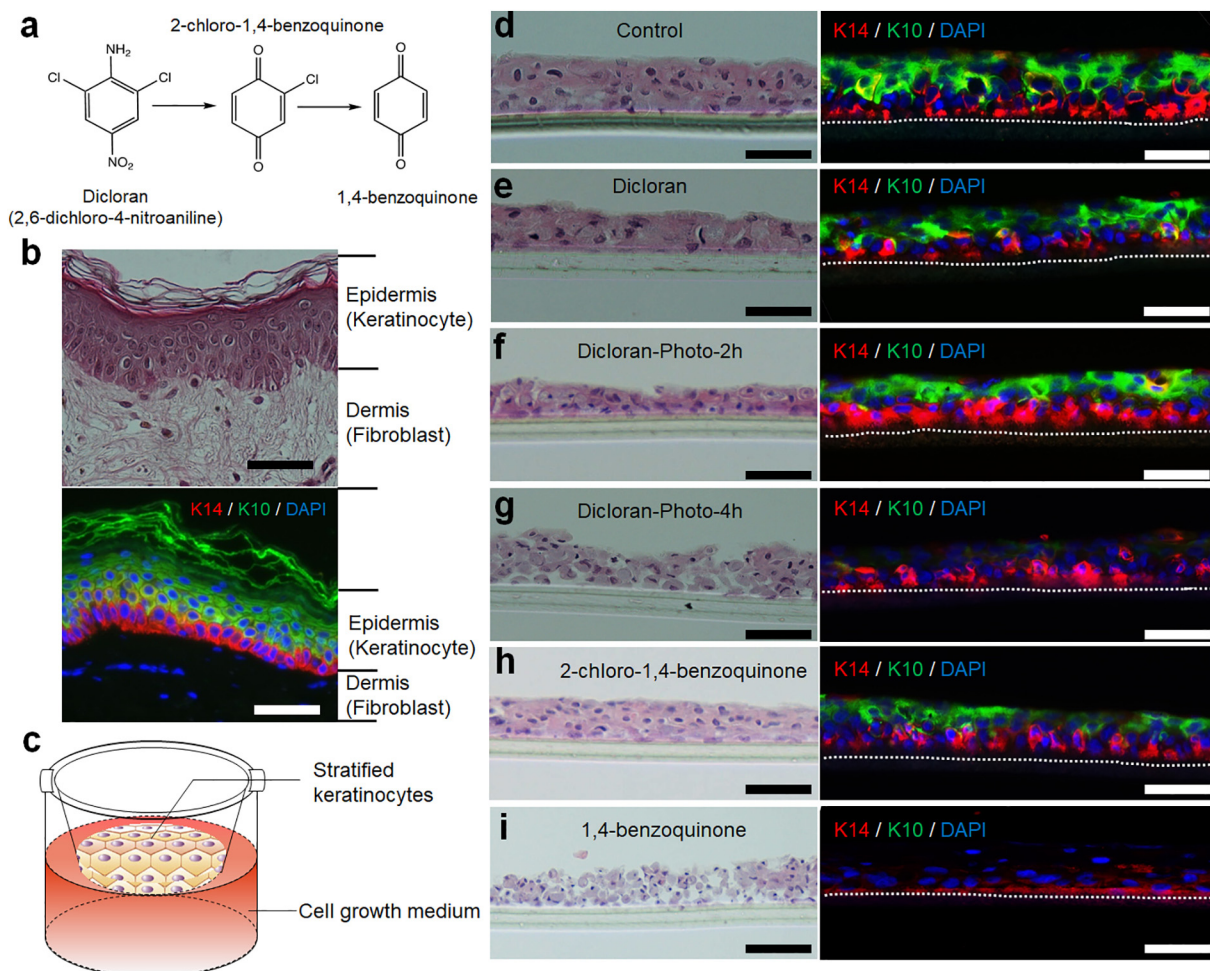


Fig. 1. Phototoxicity of dicloran and intermediate photoproducts on the differentiation of keratinocytes. Photodegradation of dicloran resulted in the generation of two intermediate products, 2-chloro-1,4-benzoquinone and 1,4-benzoquinone (a). The epidermis of normal human skin (b) was mimicked by *in vitro* stratification of keratinocytes (c). The differentiation of keratinocytes was estimated by histological H&E staining (left) and immunofluorescence (right) on the cells treated with PBS (control, d), dicloran (e), two-hour photodegraded dicloran (Dicloran-Photo-2h, f), four-hour photodegraded dicloran (Dicloran-Photo-4h, g), 2-chloro-1,4-benzoquinone (h), and 1,4-benzoquinone (i). Scale bar: 50 μ m; $n = 6$.

influence to many chemicals is ultraviolet (UV) radiation (Barron, 2007). The enhancement of chemical toxicities by UV radiation, termed phototoxicity, is by means of the degradation of chemical structures. Phototoxicity driven by UV radiation (UVR) has become a greater concern with the increase in global anthropogenic activities according to the annual reports of the United Nations Environment Programme (UNEP, 2010, 2012). As chemical phototoxicity is UVR intensity dependent, the increased intensity of UV radiation on the surface of the planet will contribute to the enhancement of chemical toxicity in the oceans (Ankley et al., 1995; Oris and Giesy, 1986). In the present investigation, we focused on the identification of potential effects of fungicide phototoxicity to human skin health.

Assessment of chemical phototoxicity has been done with many living organisms including bacteria, invertebrates, and fish (Alloy et al., 2016; Anderson et al., 1994; Guengerich et al., 1996; Incardona et al., 2012; Manzo, 2004; van de Merwe and Leusch, 2015). However, investigations on the influence of organic contaminant phototoxicity to human health are limited due to the difficulties in using human or mammalian models. As the outermost physical barrier of the human body, the skin is at most risk of exposure to a variety of chemical compounds. A number of pesticides have been reported to cause skin irritation and diseases. Farmers with long-term exposure to certain pesticides were found to have an excess risk of skin cancers (Blair and Zahm, 1995; Blair et al., 1992; Dennis et al., 2010). Many acute

inflammatory skin diseases with symptoms of redness, pain, heat, and swelling have also been reported with short-term contact with pesticides (Cole et al., 1997; Dong et al., 2013; Penagos, 2002). Despite efforts in the past decade, understanding the potential risk of human skin exposed to pesticide wastes in the environment remains largely unknown.

To establish a rapid and reliable method for the assessment of pesticide toxicities, we applied the three-dimensional (3D) human keratinocyte culture model and keratinocyte-fibroblast co-culture model to simulate natural human skin *in vitro*. The stratified multi-layer keratinocyte culture was used to simulate the different stratum layers in natural skin epidermis. Changes in barrier function of this *in vitro* keratinocyte model can be measured by evaluating the cell differentiation (Xu et al., 2014) while the activation of dermal fibroblast cells by keratinocytes can be simulated by the keratinocyte-fibroblast co-culture model (Xu et al., 2015a; Xu et al., 2015b; Zhong et al., 2016). In this study, the *in vitro* keratinocyte culture model and keratinocyte-fibroblast co-culture model were used to estimate the phototoxicity of a widely used fungicide in the Southern and Western United States, dicloran (or DCNA, 2,6-dichloro-4-nitroaniline). Although severe damage to liver, kidney, spleen, and hematopoietic system have been reported by the U.S. Environmental Protection Agency (USEPA, 2006), no studies have been done to address the potential toxicity to skin of this fungicide. The structural modifications of dicloran under photo

exposure and other environmental stresses have been documented (USEPA, 2006). Toxicity test on photodegraded dicloran with the 3D human keratinocyte culture and keratinocyte-fibroblast co-culture models provides a novel strategy to measure pesticide toxicity assessment in agriculture.

2. Methods

2.1. Cells and fungicide chemicals

All human cells used in the present study were gifts from the Laboratory for Tissue Repair & Regenerative Surgery at the Northwestern University, Feinberg School of Medicine. Two types of human cells, keratinocytes (HFKs) and dermal fibroblast cells (HFCs), both isolated from infant foreskin tissues, were used in this study. In each assay used HFKs or HFCs isolated from three pools of foreskin tissues.

The target chemicals investigated in the study included dicloran (2,6-dichloro-4-nitroaniline) and two of its intermediate photodegradation products (Fig. 1a), 2-chloro-1,4-benzoquinone (CBQ) and 1,4-benzoquinone (BQ). All chemicals were purchased from Sigma-Aldrich Co. (St. Louis, MO).

2.2. Photodegradation of dicloran in water

The photodegradation of dicloran and laboratory irradiation procedures were previously published (Vebrsky et al., 2018; Xu et al., 2018). Briefly, analytical grade dicloran was dissolved in HPLC (high-performance liquid chromatography) grade acetonitrile at 1000 mg/L. Prior to irradiation the stocking solution was diluted to 1 ppm (part per million, 1 mg/L) in distilled water in 2 mL borosilicate glass vials (Agilent Technologies, Santa Clara, CA).

The vials containing dicloran solution were incubated in an Atlas SUNTEST XXL+ environmental chamber (Mount Prospect, IL) equipped with a daylight filter. Natural sunlight was simulated at an irradiance between 300 and 400 nm wavelengths with 20% relative humidity in the chamber. The irradiance intensity was 40 W/m² which was equivalent to 1.2 h of light exposure at 30°N latitude during the June solstice (Pidwirny, 2016). The degraded samples were collected at 0, 2, and 4-hour post irradiation and the presence of products were confirmed using an Agilent 1260 Infinity HPLC (Santa Clara, CA). The solutions containing degraded dicloran were filtered with a sterile syringe filter with 0.2 μm cellulose acetate membrane (VWR International Co., Radnor, PA) and diluted with cell culture sterile phosphate buffered saline (PBS, Corning Inc., Corning, NY) at 1:50 (20 ppb) and 1:10 (100 ppb) prior to the treatment on cells.

2.3. Keratinocyte differentiation model

To mimic the natural human skin epidermis containing multi-layer differentiated keratinocytes (Fig. 1b), an *in vitro* keratinocyte stratification model was created following a previously published protocol (Xu et al., 2015a; Xu et al., 2014). The cultured human keratinocytes (HKs) were maintained in serum-free GIBCO™ Defined Keratinocyte-SFM (DK-SFM, Thermo-Fisher Scientific, Laquemeine, LA) until passage five. About a half million HKs were seeded onto a 0.4 μm tissue culture plate insert (12-mm diameter) with the polyester membrane (VWR International Co., Radnor, PA) and incubated in a 12-well plate filled with DK-SFM for 48 h at 37 °C with 5% CO₂ (Fig. 1c). Thereafter, the DK-SFM was removed from the insert and medium in the plate was replaced with the keratinocyte differentiation medium containing 50:50 (v/v) DMEM (Corning Inc.) and DMEM/F-12 (Corning Inc.) supplemented with 18 μM adenine, 500 ng/mL bovine pancreatic insulin, 500 ng/mL human Apo-transferring, 500 ng/mL triiodothyronine, 4 mM L-glutamine, 0.4 μg/mL hydrocortisone, 10 ng/mL cholera toxin, 5 ng/mL recombinant human epithelial growth factor (EGF), and 5% fetal bovine

serum (FBS). Treatment of dicloran, photodegraded dicloran (two-hour and four-hour photodegraded dicloran), or the two purified intermediate products of dicloran photodegradation (CBQ and BQ) at a concentration of 20 ppb (part per billion) or 100 ppb was applied to each cell culture sample by mixing the chemicals in the cell culture medium. Since the two-hour and four-hour photodegraded dicloran contained multiple chemicals, the two concentrations used for the treatment were the original concentrations of the dicloran prior to photodegradation. An eight-hour daily treatment was applied to each cell culture and followed by a 16-hour recovery by replacing the chemical-containing medium with fresh medium without chemical. The cells were cultured for 14 days after the start of treatment. Prior to harvest, cells were ‘starved’ with plain DMEM medium for 24 h. Cells from each treatment were preserved in 4% paraformaldehyde PBS (PFA-PBS) solution for immunofluorescence or in Invitrogen™ TRIzol RNA Isolation Reagent (Thermo-Fisher Scientific).

2.4. Keratinocyte migration model

The keratinocyte migration model has been established and used in our previous studies (Xu et al., 2014; Zhong et al., 2016). Briefly, 5 × 10⁵ keratinocytes were seeded in each well of a 12-well plate. Cells reached > 95% confluence overnight at 37 °C. Cells were then washed by PBS followed by a treatment with DK-SFM containing 10 μg/mL mitomycin C at 37 °C for 4 h. Thereafter, the medium in each well was replaced by fresh DK-SFM and a scratch through the cell monolayer was created using a 200 μL pipette tip (Thermo-Fisher Scientific). Photos of each scratch were taken at two different locations near the center of each well. Cells in each were then treated with 100 ppb of PBS (control), dicloran (DC), two-hour photodegraded dicloran (DC-PD-2h), four-hour photodegraded dicloran (DC-PD-4h), CBQ, or BQ and incubated in 37 °C for 16 h at 5% environmental CO₂. The scratch of each cell sheet was observed at similar locations and two photos were taken for each well. The size of each gap on each cell sheet was measured using ImageJ (Schneider et al., 2012) at both 0 (Fig. 3a, A₀) and 16 h (Fig. 3b, A_{16h}) post treatment. The percentage of gap closure of each scratch was calculated as 100 × (A₀ - A_{16h}) / A₀.

2.5. Keratinocyte-fibroblast co-culture model

The keratinocyte-fibroblast co-culture (KFC) model was also used and has been described in previous works (Xu et al., 2015a; Zhong et al., 2016). Keratinocytes were cultured and differentiated in cell-culture inserts for 6-well plates as described in the keratinocyte differentiation model. The HFCs were grown in the 6-well plates until the cell densities reached 50% confluence. Prior to the co-culture of the two types of cells, both HFKs and HFCs were starved by FBS-free DMEM overnight at 37 °C. Thereafter, the cell culture inserts with differentiated keratinocytes were transferred to 6-well plates containing HFCs in each well (Fig. 4a). Treatments with PBS (control), dicloran, photodegraded dicloran, and intermediate photoproducts were applied on the top of stratified keratinocytes to avoid direct stimulation of the treatment to the HFCs in each well. The treatments on keratinocytes lasted for 8 h at 37 °C followed by the complete removal of the treatment solution on the top of keratinocyte cell sheet. Thereafter, the KFC units were kept at 37 °C for 16 h. After the treatment, HFCs in each well were harvested using TRIzol (Thermo-Fisher Scientific) or were fixed in 4% PFA-PBS.

2.6. Quantitative PCR (qPCR) and immunofluorescence (IF)

The HFKs and HFCs used for qPCR were harvested using TRIzol (Thermo-Fisher Scientific). The stratified keratinocytes grown on top of cell culture insert membranes were mixed with 1 mL TRIzol containing 0.2 mL 1 mm diameter glass beads and homogenized with a vortex at 2200 rpm for 5 min. The HFCs grown in each plate were directly lysed

using 1 mL TRIzol and collected using 1.5 mL microcentrifuge tubes. The total RNAs of samples were then isolated following the protocol provided by the company. A TURBO DNA-free™ Kit (Life Technologies, Grand Island, NY) was used for DNA removal during the RNA purification step. Construction of cDNAs of RNA samples were completed using the SuperScript IV Reverse Transcriptase system (Thermo-Fisher Scientific) following the manufacturer's instructions. Primers used in this study were all previously validated in human cells and are listed in Supplementary Table 1. The qPCRs were performed using a Sybr Green system on a 7900HT Fast Real-Time PCR System with 384-Well Block Module (Thermo-Fisher Scientific) following a regular protocol. Normalizations of the raw cycle threshold (Ct) values obtained from the qPCR were done using the Ct values from a housekeeping gene, GAPDH. The relative expression of each gene in each sample was estimated using the $\Delta\Delta Ct$ method with the normalized Ct values (Livak and Schmittgen, 2001). The expression level of each gene at control condition was set to value 1 and the levels in other samples were calculated using the $\Delta\Delta Ct$ method as relative expression levels.

The IF was done with stratified keratinocytes and mono-layer HFCs. The PFA-PBS fixed HFCs on cell culture inserts were dehydrated, paraffinized, and embedded in paraffin following regular process for histological samples. Cross-sections of each embedded membrane were produced using a microtome to generate histological slides with 5 μ m thickness. One slide from each sample was stained with Hematoxylin & Eosin (H&E) to evaluate the morphology of each sample. The IFs slides with various antibodies were performed following a standard IF protocol. The histological slides of keratinocytes used for IF were deparaffinized and rehydrated prior to the IF while the PFA-PBS fixed HFCs in 6-well plates were directly used for IF analysis. The primary antibodies used on keratinocyte slides include Ki-67 (Novus Biologicals, Littleton, CO; Rabbit \times Human, 1:400 dilution), cytokeratin 14 (Thermo-Fisher Scientific; Mouse \times Human, 1:2000 dilution) and cytokeratin 10 (Novus Biologicals, Littleton, CO; Rabbit \times Human, 1:2000 dilution). The Mouse \times Human pro-collagen I α 1 (pro-CollI α 1) primary antibody was used on HFCs with a dilution 1:100 (Developmental Studies Hybridoma Bank at the University of Iowa, Iowa City, IA). Secondary antibodies conjugated with Alexa 488 (green) or 594 (red) fluorescent dye (Thermo-Fisher Scientific) were applied to slides or cell samples with a dilution of 1:500. Counter-stainings with a nuclear dye, 4',6-diamidino-2-phenylindole (DAPI, blue, 0.1 μ g/mL) were performed on samples. Photos through each color channel were taken under a Nikon Eclipse Ti fluorescent microscope (Nikon USA) and an ANDOR iXon^{EM} camera (ANDOR Technology, Concord, MA). The different color channels of each figure were merged by ImageJ (Schneider et al., 2012).

2.7. Statistical analyses

The keratinocyte cell sheet migration was evaluated using the percentage of gap closure. The production of pro-inflammatory molecules in keratinocytes was estimated by qPCR using the $2^{-\Delta\Delta Ct}$ values. The activation of HFCs co-cultured with keratinocytes was measured using qPCR of pro-CollI α 1 and α -SMA, and the average signal intensity of pro-CollI α 1 in each IF image. The digitalization of signal intensities was done using ImageJ and the average signal intensity of pro-CollI α 1 in each image was calculated as (Xu et al., 2015a; Zhong et al., 2016):

$$\text{Average expression level of proColl}\alpha 1 = \frac{\text{Total signal intensity of the image}}{\text{Total number of the cells in the image}}$$

The distributions of all data were analyzed using Shapiro–Wilk test (David and Johnson, 1951) for the normality test of the datasets. All datasets were also evaluated with Bartlett's test (Bartlett, 1937) to test the homogeneity of data variance. All datasets from different analyses were confirmed to be good for the ANOVA tests according to the results

of Shapiro–Wilk and Bartlett's tests. Multiple comparisons between treatment and control groups were performed using one-way or two-way ANOVA and Tukey's tests with least-squares means. The adjusted *p*-values generated from the statistical tests were used to demonstrate the significance of the difference between treatment and control groups.

3. Results

3.1. Differentiation of keratinocytes was compromised by the photodegraded dicloran and purified intermediates

The photodegradation of dicloran has been reported previously (Vebrosky et al., 2018). Two major intermediate products, 2-chloro-1,4-benzoquinone (CBQ) and 1,4-benzoquinone (BQ), were detected during the degradation of dicloran (Fig. 1a). Under normal growing conditions, the human epidermis contains multiple keratinocyte layers with cytokeratin markers differentially expressed in different layers (Fig. 1b). In the present study, an *in vitro* artificial epidermis model containing several layers of keratinocytes was created on the membrane of a cell culture insert (Fig. 1c). Similar to the epidermis in the natural human skin, the artificial stratified keratinocytes under controlled conditions contained 5–6 layers of keratinocytes (Fig. 1d). The expression patterns of cytokeratin (CK) 10 and 14 in the *in vitro* model were also similar to those in real epidermis: the CK14 was primarily expressed along the basal layer of keratinocytes while the CK10 dominated the suprabasal layers (Fig. 1b and d). The concentrations of the chemicals used in this study were tested on mono-layer keratinocyte cultures prior to application to the stratified keratinocytes. No chemical significantly influenced cell proliferation at concentrations up to 100 ppb in cell culture medium (Suppl. Fig. 1).

Daily applications of dicloran at a concentration of 100 ppb did not result in a significant effect on differentiation since multiple layers of keratinocytes with clearly separated CK expression patterns were observed (Fig. 1e). Similarly, two-hour photodegraded dicloran (DC-PD-2h) also showed a minimum impact on keratinocyte differentiation. Although a thinner artificial epidermis was observed on the keratinocytes treated with DC-PD-2h, no significant effects were seen in the expression patterns of CK10 and 14 in this group (Fig. 1f). A severe inhibitive effect on keratinocyte *in vitro* differentiation was observed in the keratinocytes treated with four-hour photodegraded dicloran (DC-PD-4h). The alignment of cells in each layer was morphologically disrupted and the expression of CK10 in suprabasal layers of keratinocytes was also diminished (Fig. 1g). The outcomes of the keratinocyte differentiation treated with CBQ and BQ were distinct. While no clear influence was observed in the artificial epidermis with CBQ treatment (Fig. 1h), the keratinocytes under treatment of BQ demonstrated attenuated differentiation with poorly aligned cells and minimum expression levels of CK 14 and 10 (Fig. 1i).

3.2. Photodegraded dicloran and intermediate products induced the expression of pro-inflammatory related genes

The expression patterns of 17 pro-inflammatory related genes under stimulations of dicloran and its photoproducts were tested using qPCR. The genes were identified as major players involved in pro-inflammatory responses in skin epidermis in one of our earlier studies (Xu et al., 2014). Based on their expression profiles, these 17 genes were classified into three groups as shown in the heatmap (Fig. 2a). Genes C-C motif chemokine ligand 4 (*ccl4*), C-X-C motif chemokine ligand 2 (*cxcl2*), interleukin 6 (*il6*), and matrix metalloproteinase 9 (*mmp9*) demonstrated significantly upregulated expression levels (> 200% of control with *p* < 0.05) with stimulation of one or more chemicals. Setting the expression levels of all genes in control cells as value 1, the relative expression level of *ccl4* in the cells treated with 100 ppb BQ reached to 5.27 ± 1.25 (*p* < 0.0001, Fig. 2b and Suppl Table 2). The expression of *cxcl2* in keratinocytes was inducible by dicloran-photo-2h

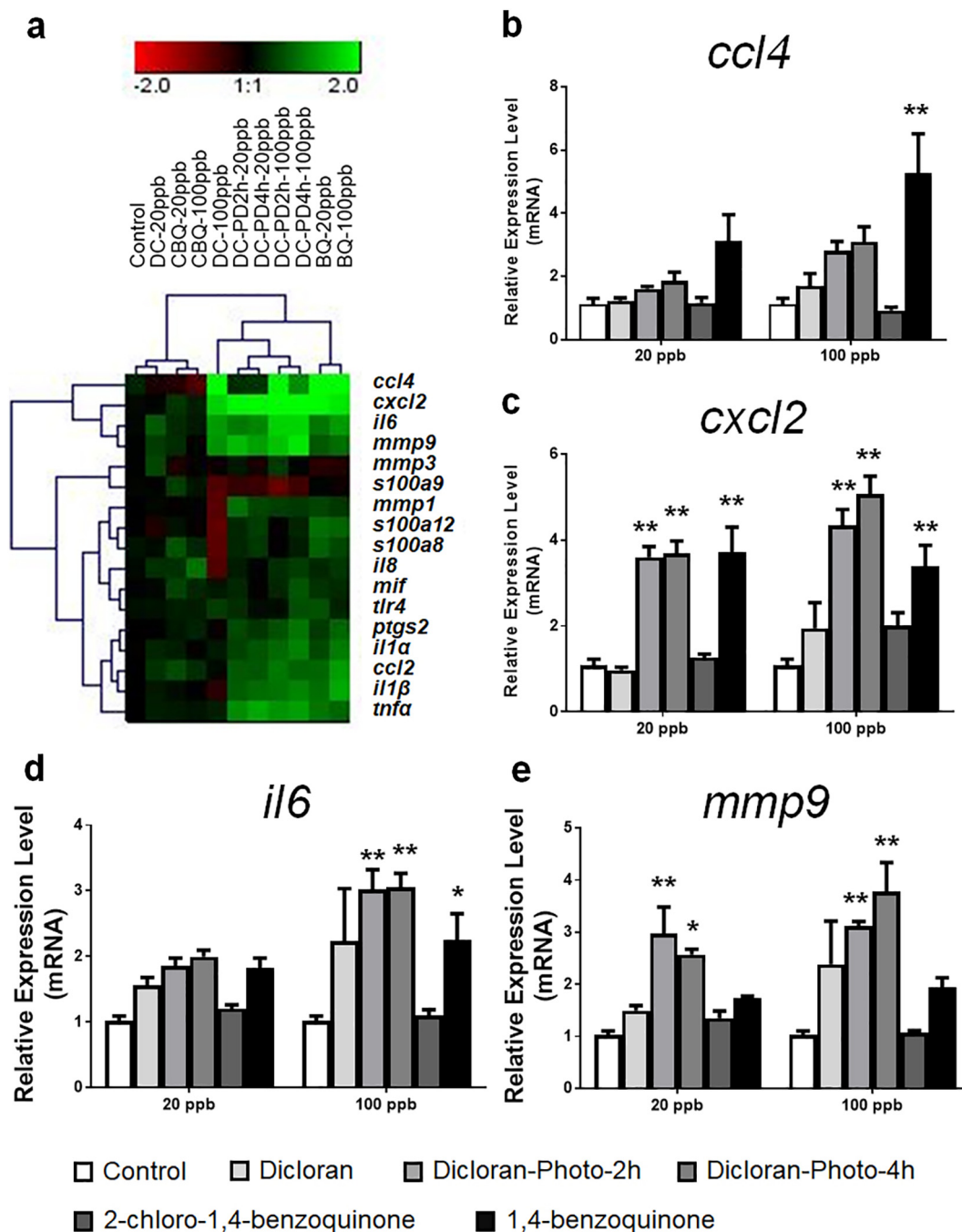


Fig. 2. Production of pro-inflammatory molecules by differentiated keratinocytes. Expression levels of 17 pro-inflammatory protein-encoding genes were evaluated by qPCR. The overall expression patterns of these genes (green: upregulated compared to control; red: downregulated compared to control) were clustered based on the qPCR results (a). The expression profiles of CCL4 (b), CXCL2 (c), IL-8 (d), and MMP-6 (e) in keratinocytes under stress of dicloran, photodegraded dicloran, and the two intermediate photoproducts were demonstrated. * $0.01 < p < 0.05$; ** $p < 0.01$. $n = 8$. (For interpretation of the references to color in this figure legend, the reader is referred to the web version of this article.)

(3.61 ± 0.25 , $p < 0.0001$), dicloran-photo-4h (3.69 ± 0.29 , $p < 0.0001$), and BQ (3.72 ± 0.59 , $p < 0.0001$) at 20 ppb. Similar upregulation of *cxcl2* was also found in the keratinocytes incubated with 100 ppb dicloran-photo-2h, dicloran-photo-4h, and BQ with relative expression levels at 4.34 ± 0.37 ($p < 0.0001$), 5.07 ± 0.42 ($p < 0.0001$), and 3.34 ± 0.50 ($p = 0.0003$), respectively (Fig. 2c). The cytokine *il6* (Fig. 2d) only showed elevated expression levels in response to the induction of 100 ppb dicloran-photo-2h (3.02 ± 0.30 , $p < 0.0001$), dicloran-photo-4h (3.05 ± 0.22 , $p < 0.0001$), and BQ (2.24 ± 0.41 , $p = 0.042$). Both dicloran-photo-2h and dicloran-photo-4h enhanced the production of *mmp9* at mRNA levels in keratinocytes

compared to in control cells (Fig. 2e). The dicloran-photo-2h elevated the mRNA levels of *mmp9* to 2.98 ± 0.51 ($p = 0.0012$) and 3.12 ± 0.08 ($p = 0.0004$) with concentrations at 20 and 100 ppb, respectively. The dicloran-photo-4h increased the *mmp9* at transcription level to 2.57 ± 0.10 (0.019) and 3.78 ± 0.56 ($p < 0.0001$) with 20 and 100 ppb, respectively.

The second group of genes including prostaglandin-endoperoxide synthase 2 (*ptgs2*), interleukin 1 α (*il1a*), C-C motif chemokine ligand 2 (*ccl2*), interleukin 1 β (*il1b*), and tumor necrosis factor α (*tnfa*), demonstrated less upregulation in transcriptomic levels upon stimulation of chemicals, compared to the first group of genes. The expression

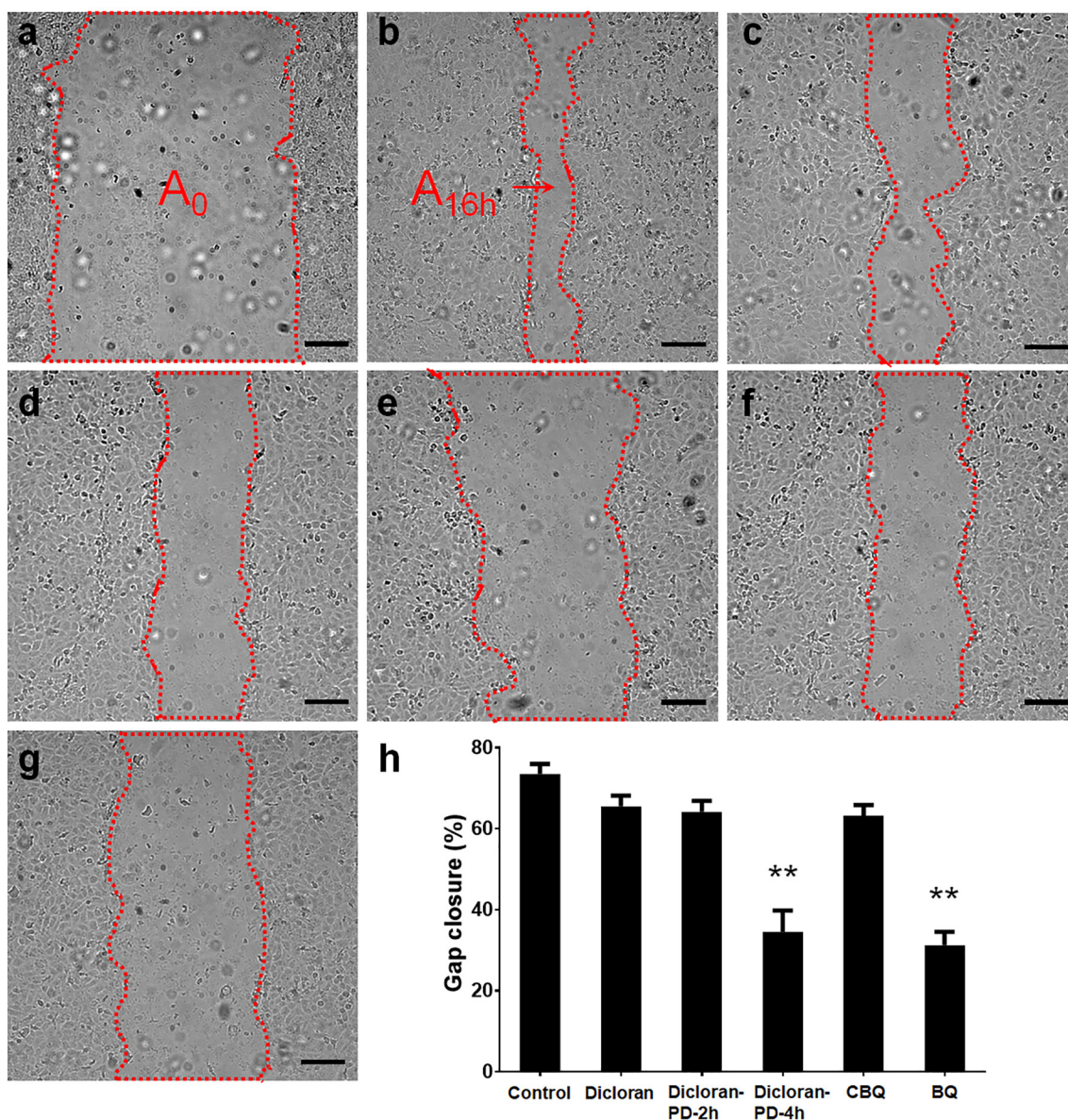


Fig. 3. Keratinocyte migration with the treatment of dicloran, photodegraded dicloran, and intermediate photoproducts. Scratches were made on the mono-layer keratinocytes and the photos of the scratches were taken before any treatments with chemicals (a). The scratch of each cell sheet treated with PBS (control, b), dicloran (c), two-hour photodegraded dicloran (DC-PD2h, d), four-hour photodegraded dicloran (DC-PD4h, e), 2-chloro-1,4-benzoquinone (CBQ, f), or 1,4-benzoquinone (BQ, g) was taken 16 h after the application of treatment. The percentage of the gap closure for each sample was calculated and graphed (h). A₀: area of the gap prior to the treatment (the area enclosed by the dashed line); A_{16h}: area of the gap 16 h post-treatment. Scale bar: 50 μ m. ** $p < 0.01$. $n = 12$.

profiles of this group of genes suggested that they were also inducible by at least one of the chemicals used in this study with statistical significance ($p < 0.05$, Suppl Fig. 1 and Suppl Table 2). In contrast, the third group of genes, which contained interleukin 8 (*il8*), matrix metalloproteinase 1 and 3 (*mmp1* and *mmp3*), S100 calcium binding protein A8, A9, A12 (*s100a8*, *s100a9*, and *s100a12*), and toll-like receptor 4 (*tlr4*), did not show significantly meaningful up- or down-regulation with the treatment of any chemicals (Suppl Fig. 1 and Suppl Table 2).

3.3. Photodegraded dicloran and intermediate products inhibited the migration of keratinocytes in vitro

The keratinocytes incubated with dicloran and its photodegradation-related chemicals demonstrated different abilities in migration. The keratinocyte migration assay was performed using the cell sheet scratch assay (Fig. 3a). In control samples, $73.51 \pm 2.45\%$ of the gap created on the surface of the cell sheet was closed by the migration of

keratinocytes after 16-hour incubation (Fig. 3b). Application of 100 ppb dicloran or dicloran-photo-2h to the keratinocytes during gap closure did not significantly change the percentages of the closure after 16-hour cell migration. About $65.51 \pm 2.66\%$ (Fig. 3c, $p = 0.529$ compared to the control) of the gap was filled by keratinocytes treated with dicloran while $64.16 \pm 2.67\%$ (Fig. 3d, $p = 0.353$ compared to the control) gap on the cell sheet incubated with dicloran-photo-2h was closed within 16 h. However, keratinocytes treated with dicloran-photo-4h demonstrated a significant delay in cell migration ($p < 0.0001$ compared to the control), which resulted in only $34.51 \pm 5.25\%$ gap closure within 16 h (Fig. 3e). The two intermediate products of dicloran photodegradation showed different effects on keratinocyte migration. Treated with 100 ppb CBQ, the keratinocytes recolonized $63.23 \pm 2.62\%$ of the original gap ($p = 0.252$ compared to the control, Fig. 3f). In contrast, the keratinocytes treated with 100 ppb BQ recovered only $31.23 \pm 3.29\%$ of the gap after 16-hour migration ($p < 0.0001$ compared to the control, Fig. 3g). The quantification of

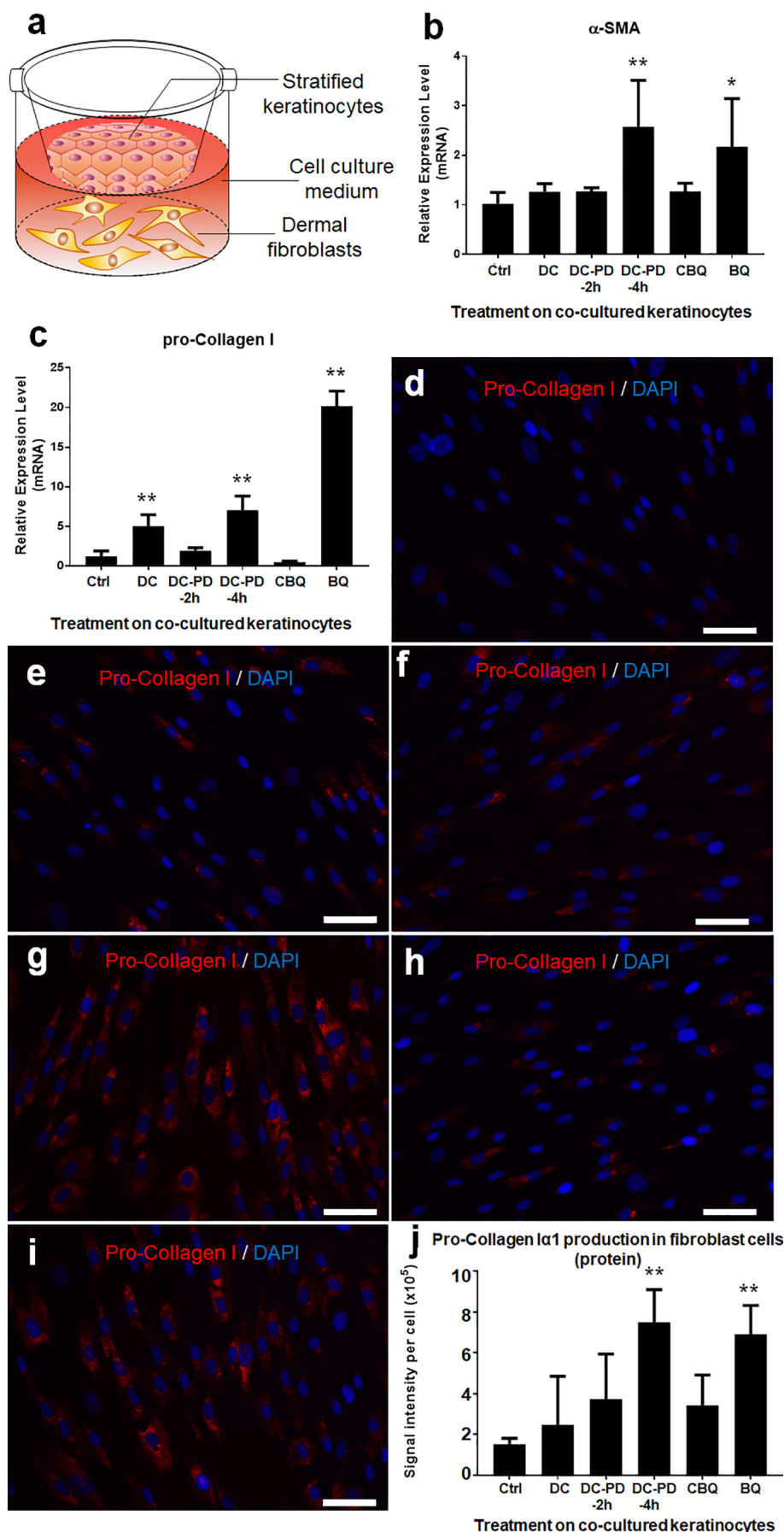


Fig. 4. Activation of dermal fibroblasts co-cultured with keratinocytes treated with different chemicals. The human keratinocytes and fibroblast cells were co-cultured using transwell cell culture inserts in six-well plates (a). Activation of dermal fibroblasts was evaluated by the relative expression levels of α smooth muscle actin (α -SMA, b) and pro-collagen I (pro-Col I, c) using qPCR. The protein level of pro-Col I was visualized by immunofluorescent microscopy using the dermal fibroblasts co-cultured with the keratinocytes under the stress of PBS (control, d), dicloran (e), two-hour photodegraded dicloran (DC-PD-2h, f), four-hour photodegraded dicloran (DC-PD-4h, g), 2-chloro-1,4-benzoquinone (CBQ, h), or 1,4-benzoquinone (BQ, i). The fluorescent signals were quantified using ImageJ (j).

gap closure for cells with different treatments is shown in Fig. 3h.

3.4. HFKs responded to photodegraded dicloran and intermediate products manipulated the status of HFCs

To evaluate the effects of chemicals on simulated epidermal keratinocytes on the fibroblast cells in the dermis, a KFC model was created (Fig. 4a). In this model, a monolayer of HFCs was cultured in six-well plates underneath the cell culture inserts with stratified HFKs on the top of membranes. The wells were filled with cell culture medium, which served as the extracellular matrix. This allowed the interactions between HFKs and HFCs. Since the epidermis was likely to be exposed to chemicals in water, treatments of dicloran and related products were only applied to the top of fully stratified HFKs. During the incubation, no dicloran or any other photodegraded dicloran products were detected in the cell culture medium in each well (data not shown), which suggested that there were no direct chemical effects on HFCs.

Incubated with the HFKs with various chemical treatments, the HFCs were differentially activated based on the production of α -SMA (*acta2*) and pro-Collagen I α 1 (*col1a1*) at mRNA and protein levels. Higher mRNA levels of *acta2* were identified in the HFCs co-cultured with the HFKs treated with 100 ppb DC-PD-4h (2.58 ± 0.38 , $p = 0.0006$ compared to HFCs co-cultured with HFKs in control condition) or BQ (2.18 ± 0.40 , $p = 0.0159$ compared to HFCs co-cultured with HFKs in control condition). Similarly, the mRNA levels of *col1a1* in HFCs co-cultured with 100 ppb DC-PD-4h (5.04 ± 0.74 , $p < 0.0001$) or BQ (20.16 ± 0.77 , $p < 0.0001$). In addition, the 100 ppb dicloran treated HFKs also elevated the mRNA level of *col1a1* to 5.04 ± 0.59 ($p = 0.0002$). Production of pro-Collagen I α 1 by HFCs at protein level also showed similar patterns as in the mRNA level. The production of pro-Collagen I α 1 in the HFCs co-cultured with HFKs with treatment of control (Fig. 4d), dicloran (Fig. 4e), DC-PD-2h (Fig. 4f), and CBQ (Fig. 4h) were low with average signal intensities at $1.52 \pm 0.17 \times 10^5$, $2.47 \pm 1.38 \times 10^5$, $3.74 \pm 1.27 \times 10^5$, and $3.42 \pm 0.86 \times 10^5$ per cell (Fig. 4j), respectively. In contrast, the production of pro-Collagen I α 1 in HFCs were significantly enhanced by co-cultured HFKs stimulated by DC-PD-4h (Fig. 4g) and BQ (Fig. 4i), with the average signal intensities reach $7.50 \pm 0.80 \times 10^5$ and $6.92 \pm 0.70 \times 10^5$ per cell, respectively. This suggested that the HFKs in response to stimulation of DC-PD-4h and BQ were more likely to activate HFCs grown in the same medium.

To further rule out the direct effects of the chemicals on HFCs, HFCs were grown in new six-well plates without the presence of HFKs. The HFCs were treated with PBS (control), dicloran, DC-PD-2h, DC-PD-4h, CBQ, and BQ at 100 ppb in the medium for 8 h and further incubated in fresh medium for 16 h. By analyzing the expression profiles of *acta2* and *col1a1* at mRNA and protein levels, we did not identify any difference between any direct chemical treatments; this indicated that the activation of HFCs was mediated by co-cultured HFKs rather than the chemicals (Suppl Fig. 3).

4. Discussion

As the first physical barrier of the human body, the skin comes easily into contact with all kinds of chemicals in the environment, including the contaminants in water or through exposure of a worker who is applying the chemical. With the release of agrochemicals into water from agricultural activities, the risk of the skin exposure to harmful agricultural wastes is likely. A number of pesticides have been shown to illicit toxic effects to humans following direct exposure. This can occur through entry into the bloodstream by penetrating the skin directly damaging the skin itself resulting in cutaneous toxicity (Urban and Anadkat, 2013). Because of the potential threats to human skin health, human health risk evaluations include recommended cutaneous toxicity tests for pesticide registration (FDA, 2015a, 2015b). It is also mandatory to provide critical information about the pesticide in the label of

the product, such as major chemical compounds, direction for handling, and alert signals for users (Settivari et al., 2015). Many of these agrochemicals are designed to be less stable so that the residues in the environment will dissipate within a short period of time. This is a common strategy to minimize the environmental contamination caused by these chemicals. However, it may also result in some unpredictable toxicities to organisms by the degraded products. The chemical that was tested in the present study, has been previously reported as a non-stable compound under UV exposure (Vebrosky et al., 2018); dicloran and its photodegradation products demonstrated different toxicities to the cardiomyocytes of the eastern oysters (Xu et al., 2018).

In this study, changes in dicloran toxicity to human skin cells were also observed following UV exposure. After four-hour irradiation, dicloran demonstrated significant impacts on human keratinocyte differentiation, migration, and amplified the activation of human dermal fibroblast cells through keratinocytes. Interestingly, the keratinocytes treated with one of the major dicloran photodegradation intermediate products, 1,4-benzoquinone, behaved similarly to the cells treated with four-hour photodegraded dicloran. The dynamic profile of dicloran photodegradation in water in our previous study showed that the 1,4-benzoquinone is one of the dominant intermediate products after four-hour degradation. Commonly known as para-quinone, the 1,4-benzoquinone has been reported to cause skin erythema, which is related to skin inflammation (USDHHS, 1993). The other intermediate product of dicloran photodegradation, 2-chloro-1,4-benzoquinone, did not show any notable effects on keratinocytes, which suggests that this chemical may be less toxic to human skin. Similarly, the two-hour photodegraded dicloran, containing the 2-chloro-1,4-benzoquinone as one of the dominant compounds, did not significantly affect the keratinocytes in differentiation, migration, or fibroblast cell activation. Although a small amount of 1,4-benzoquinone was also detected in the two-hour photodegraded dicloran, it was unlikely to stimulate the keratinocytes with such a low concentration at 24 ppb (Vebrosky et al., 2018; Xu et al., 2018).

The keratinocyte assays used in the present study were all well-accepted methods for *in vitro* studies in skin injuries and diseases. The differentiation of keratinocytes determines the stratification of epithelium in the epidermis (Fuchs and Raghavan, 2002). During the differentiation, the cytokeratin markers expressed in the keratinocytes are shifted from CK5 and 14 in the basal layer to CK1 and 10 in suprabasal layers (Darmon and Blumenberg, 1993). The abnormal keratinocyte differentiation is a hallmark of some common skin inflammatory disorders, such as atopic dermatitis and psoriasis (Wikramanayake et al., 2014). Associated with the barrier perturbation resulted from the interrupted keratinocyte differentiation in the epidermis, elevated cytokine production, such as TNF- α , IL-1 α , and 1 β , has also been identified in skin inflammatory diseases (Segre, 2006). The cytokines released by keratinocytes in the epidermis contribute to the cell differentiation in an autocrine pathway and also trigger the inflammatory responses through paracrine and endocrine pathways (Wikramanayake et al., 2014). The upregulation of these cytokines by photodegraded dicloran were also identified in our study, suggesting that the photoproducts of dicloran and the intermediate chemical, 1,4-benzoquinone, potentially resulted in the epidermal inflammation in human skin.

The expression levels of several pro-inflammatory cytokine genes, including *tnfa*, *il1a*, *il1b*, *il6*, and *mif*, were investigated in keratinocytes under the stimulation of various chemicals. The influence of photodegraded dicloran and 1,4-benzoquinone on the expression of *il6* was the most significant, followed by *tnfa*, *il1a*, and *il1b*, which showed fewer responses to the stimulation of the tested chemicals. The IL-6 mediates a wide range of inflammatory diseases (Turksen et al., 1992) and is critical to growth and differentiation of various cell types (Audet et al., 2001). Studies on IL-6 indicates that this molecule plays a key role in a number of skin diseases, such as psoriasis (Bonifati et al., 1994; Castells-Rodellas et al., 1992) and lupus erythematosus (Nurnberg et al., 1995). Upregulation of *il6* expression has also been observed in

skin suffering from barrier disruption and the repair of barrier repair in *il6* knockout mice (*il6*^{-/-}) is significantly delayed (Wang et al., 2004). An increase of epidermal expression of *il1a* and *il1b* was also observed upon acute skin barrier disruption in an earlier study (Wood et al., 1992). The production of cytokine IL-1 α and IL-1 β mediates the epidermal differentiation in response to skin mechanical injuries and skin diseases (Dinarello, 2009; Groves et al., 1995; Kirschner et al., 2009). Similarly, high levels of TNF- α is correlated with acute skin barrier damage (Wood et al., 1992), especially in skin with severe psoriasis (Bonifati et al., 1994). Overexpression of *tnfa* in the epidermis prevents the recovery of the skin barrier, therefore, therapeutic strategies in reducing the TNF- α levels in the skin of psoriasis patients significantly relieve the symptoms (Lowe et al., 2007).

The photodegraded dicloran also induced the expression of a number of chemokines, including *ccl2*, *ccl4*, and *cxcl2*, in keratinocytes. Similar to the cytokines described above, chemokines are also involved in psoriasis, atopic dermatitis, and other inflammatory skin diseases. High levels of CCL2, CCL4, and CXCL2 have been identified in the skin lesions of psoriasis patients (Nomura et al., 2003). The CCL2 (also known as monocyte chemoattractant protein 1, MCP-1) has been characterized as a recruiter for leukocytes in the skin through chemotactic cytokine network (Gillitzer et al., 1993). Although the exact role in skin inflammation has not been identified, CCL4 is likely to be the chemoattractant to the CCR1 or CCR5 receptor-bearing cells, such as NK cells, dendritic cells, monocytes, and Th1 cells (Nedoszytko et al., 2014). These chemokines in human keratinocytes were inducible by photodegraded dicloran and 1,4-benzoquinone at concentrations as low as 20 ppb, which suggests that the inflammatory responses caused by the chemoattracted leukocytes may be initiated in the human skin exposed to the degraded dicloran.

Other genes with inducible expression profiles by photodegraded dicloran included *mmp9* and *ptgs2*. Unlike the cytokines and chemokines that function as mediator in the upstream of inflammatory regulation, the protein products of *mmp9* and *ptgs2* encoding enzyme proteins participate in the downstream regulation of inflammation. As a family of Zn-dependent metalloproteinases, the MMPs are implicated in the different stages of skin barrier repair, such as reepithelialization, inflammatory matrix remodeling, and neovascularization (Orfanos et al., 1997; Papakonstantinou et al., 2005; Visse and Nagase, 2003). Many MMPs can be produced by keratinocytes, dermal fibroblast cells, and Langerhans cells in human skin, and they play a key role in inflammatory skin damage (Ratzinger et al., 2002; Sawicki et al., 2005). Among these MMPs, MMP-9 has been reported by several studies as a protein with an essential role in allergic skin diseases, such as atopic dermatitis (Devillers et al., 2007) and chronic urticaria (Kessel et al., 2005), which makes the MMP-9 an efficient biomarker for these skin diseases (Altrichter et al., 2009). Also known as cyclooxygenase 2 (COX-2), the PTGS2 produces prostaglandins in a wide range of inflammatory reactions. Although mostly known as an enzyme involved in skin cancers, PTGS2 was also identified as a key molecule in response to the inflammatory stimulus during skin wound repair (Wu, 1996). The prostaglandins produced by PTGS2 regulate skin inflammation through the induction of vascular permeability and infiltration of inflammatory cells (Wilgus et al., 2000). Therefore, modification of *ptgs2* expression may result in a different phenotype in skin barrier repair.

The common role of all the protein products described above is as the mediator for inflammatory response, which is the cause of many skin diseases. Upregulation of all these genes was observed in our study in response to the stimulation of photodegraded dicloran products, suggesting that exposure to photodegraded dicloran may result in damage to the skin barrier. Although it is difficult to evaluate or predict the extent of damage caused by exposure to dicloran and its photodegraded products on the real human skin, *in vitro* assays with human keratinocytes and dermal fibroblast cells can be alternative tools for assessment of their potential phototoxicity. The three-dimensional keratinocyte culture model creates the stratified epidermal layer of

human skin, which contains keratinocytes with different differentiation levels in different layers. Differentiation of keratinocytes determines the barrier function and the permeability of the epidermis. The keratinocyte scratch assay was used to test the cell migration, which is required for re-epithelialization upon injury to the skin barrier. Delay of keratinocyte migration indicates the compromised function in skin barrier recovery.

The co-culture model of keratinocytes-fibroblast cells was used in our study to understand potential effects of keratinocytes, under stimulation of dicloran photoproducts, on co-cultured fibroblast cells. Because of the release of pro-inflammatory molecules by keratinocytes stimulated by dicloran photoproducts, the dermal fibroblast cells grown in the same medium are likely to be activated. Activated dermal fibroblast cells (myofibroblasts) are often observed in the dermis undergoing re-construction of the matrix following skin injuries. Increased dermal fibroblast cell activation by keratinocytes treated with dicloran photoproduct suggested that the photodegraded dicloran indirectly influenced the remodeling of dermal matrix. In addition, the released pro-inflammatory molecules by keratinocytes are likely to manipulate the behaviors of other types of cells, such as neutrophils, macrophages, endothelial cells, etc., to initiate the inflammation in the skin.

The phototoxicity of dicloran on skin keratinocytes resulted in attenuated cell differentiation, delayed cell migration, increased production of pro-inflammatory molecules, and the enhanced ability to activate co-cultured dermal fibroblast cells. Similar effects in human skin are likely to cause skin barrier disruption, which is associated with inflammatory skin diseases. Therefore, environmental exposure to dicloran may cause skin damage through sunlight activation.

5. Conclusions

The impacts of dicloran and its photodegraded products were evaluated with the *in vitro* keratinocyte culture and keratinocyte-fibroblast co-culture model. Among all the tested chemicals, the four-hour photodegraded dicloran and 1,4-benzoquinone demonstrated the greatest toxicity in the cell culture models, which were reflected by the differentiation, migration, pro-inflammatory factor production, and dermal fibroblast activation of the keratinocytes. These changes suggested a typical inflammatory reaction in the keratinocytes. This indicated an enhanced toxicity of dicloran by photoactivation. The phototoxicity of dicloran is likely to cause acute skin inflammatory diseases in human skin.

Declaration of interests

None.

Acknowledgments

We would like to thank Dr. Seok Jong Hong from the Northwestern University, Feinberg School of Medicine for the primary cultures of infant foreskin keratinocytes and dermal fibroblast cells. The study was supported by the Internal Grant of Texas A&M University Corpus Christi.

Appendix A. Supplementary data

Supplementary data to this article can be found online at <https://doi.org/10.1016/j.envint.2018.10.010>.

References

- Alloy, M., Baxter, D., Stieglitz, J., Mager, E., Hoenig, R., Benetti, D., Grosell, M., Oris, J., Roberts, A., 2016. Ultraviolet radiation enhances the toxicity of deepwater horizon oil to Mahi-mahi (*Coryphaena hippurus*) embryos. *Environ. Sci. Technol.* 50, 2011–2017.

- Altrichter, S., Boodstein, N., Maurer, M., 2009. Matrix metalloproteinase-9: a novel biomarker for monitoring disease activity in patients with chronic urticaria patients? *Allergy* 64, 652–656.
- Anderson, S.L., Hose, J.E., Knezovich, J.P., 1994. Genotoxic and developmental effects in sea urchins are sensitive indicators of effects of genotoxic chemicals. *Environ. Toxicol. Chem.* 13, 1033–1041.
- Ankley, G.T., Erickson, R.J., Phipps, G.L., Mattson, V.R., Kosian, P.A., Sheedy, B.R., Cox, J.S., 1995. Effects of light intensity on the phototoxicity of fluoranthene to a benthic macroinvertebrate. *Environ. Sci. Technol.* 29, 2828–2833.
- Audet, J., Miller, C.L., Rose-John, S., Piret, J.M., Eaves, C.J., 2001. Distinct role of gp130 activation in promoting self-renewal divisions by mitogenically stimulated murine hematopoietic stem cells. *Proc. Natl. Acad. Sci. U. S. A.* 98, 1757–1762.
- Barron, M.G., 2007. Sediment-associated phototoxicity to aquatic organisms. *Hum. Ecol. Risk Assess.* 13, 317–321.
- Bartlett, M.S., 1937. Properties of sufficiency and statistical tests. *Proc. R. Soc. Lond. A* 160, 268–282.
- Blair, A., Zahm, S.H., 1995. Agricultural exposures and cancer. *Environ. Health Perspect.* 103 (Suppl. 8), 205–208.
- Blair, A., Zahm, S.H., Pearce, N.E., Heineman, E.F., Fraumeni Jr., J.F., 1992. Clues to cancer etiology from studies of farmers. *Scand. J. Work Environ. Health* 18, 209–215.
- Bonifati, C., Carducci, M., Cordiali Fei, P., Trento, E., Sacerdoti, G., Fazio, M., Ameglio, F., 1994. Correlated increases of tumour necrosis factor- α , interleukin-6 and granulocyte monocyte-colony stimulating factor levels in suction blister fluids and sera of psoriatic patients—relationships with disease severity. *Clin. Exp. Dermatol.* 19, 383–387.
- Castells-Rodellas, A., Castell, J.V., Ramirez-Bosca, A., Nicolas, J.F., Valcuende-Cavero, F., Thivolet, J., 1992. Interleukin-6 in normal skin and psoriasis. *Acta Derm. Venereol.* 72, 165–168.
- Cole, D.C., Carpio, F., Math, J.J., Leon, N., 1997. Dermatitis in Ecuadorean farm workers. *Contact Dermatitis* 37, 1–8.
- Darmon, M., Blumenberg, M., 1993. *Molecular Biology of the Skin: The Keratinocyte*. Academic Press, New York, NY.
- David, F.N., Johnson, N.L., 1951. The effect of non-normality on the power function of the F-test in the analysis of variance. *Biometrika* 38, 43–57.
- DeLorenzo, M.E., Wallace, S.C., Danese, L.E., Baird, T.D., 2009. Temperature and salinity effects on the toxicity of common pesticides to the grass shrimp, *Palaemonetes pugio*. *J. Environ. Sci. Health B* 44, 455–460.
- Dennis, L.K., Lynch, C.F., Sandler, D.P., Alavanja, M.C., 2010. Pesticide use and cutaneous melanoma in pesticide applicators in the agricultural heath study. *Environ. Health Perspect.* 118, 812–817.
- Devillers, A.C., van Toorenbergen, A.W., Klein Heerenbrink, G.J., Mulder, P.G., Oranje, A.P., 2007. Elevated levels of plasma matrix metalloproteinase-9 in patients with atopic dermatitis: a pilot study. *Clin. Exp. Dermatol.* 32, 311–313.
- Dinarelli, C.A., 2009. Immunological and inflammatory functions of the interleukin-1 family. *Annu. Rev. Immunol.* 27, 519–550.
- Dong, H., Peng, X., Qiu, Z., 2013. A rare case of bullous contact dermatitis caused by severe organophosphorus pesticides poisoning. *Int. J. Dermatol.* 52, 1533–1534.
- FDA, 2015a. In: Services U.S.D.o.H.a.H. (Ed.), *Nonclinical Safety Evaluation of Reformulated Drug Products and Products Intended for Administration by an Alternate Route*. Food and Drug Administration, Silver Spring, MD.
- FDA, 2015b. In: Services U.S.D.o.H.a.H. (Ed.), *S10 Photosafety Evaluation of Pharmaceuticals*. Food and Drug Administration, Silver Spring, MD.
- Fuchs, E., Raghavan, S., 2002. Getting under the skin of epidermal morphogenesis. *Nat. Rev. Genet.* 3, 199–209.
- Gillitzer, R., Wolff, K., Tong, D., Muller, C., Yoshimura, T., Hartmann, A.A., Stingl, G., Berger, R., 1993. MCP-1 mRNA expression in basal keratinocytes of psoriatic lesions. *J. Invest. Dermatol.* 101, 127–131.
- Groves, R.W., Mizutani, H., Kieffer, J.D., Kupper, T.S., 1995. Inflammatory skin disease in transgenic mice that express high levels of interleukin 1 alpha in basal epidermis. *Proc. Natl. Acad. Sci. U. S. A.* 92, 11874–11878.
- Guengerich, F.P., Gillam, E.M., Shimada, T., 1996. New applications of bacterial systems to problems in toxicology. *Crit. Rev. Toxicol.* 26, 551–583.
- Incardona, J.P., Vines, C.A., Linbo, T.L., Myers, M.S., Sloan, C.A., Anulacion, B.F., Boyd, D., Collier, T.K., Morgan, S., Cherr, G.N., Scholz, N.L., 2012. Potent phototoxicity of marine bunker oil to translucent herring embryos after prolonged weathering. *PLoS One* 7, e30116.
- Kessel, A., Bishara, R., Amital, A., Bamberger, E., Sabo, E., Grushko, G., Toubi, E., 2005. Increased plasma levels of matrix metalloproteinase-9 are associated with the severity of chronic urticaria. *Clin. Exp. Allergy* 35, 221–225.
- Kirschner, N., Poetzl, C., von den Driesch, P., Wladykowski, E., Moll, I., Behne, M.J., Brandner, J.M., 2009. Alteration of tight junction proteins is an early event in psoriasis: putative involvement of proinflammatory cytokines. *Am. J. Pathol.* 175, 1095–1106.
- Livak, K.J., Schmittgen, T.D., 2001. Analysis of relative gene expression data using real-time quantitative PCR and the $2^{-\Delta\Delta CT}$ method. *Methods* 25, 402–408.
- Lowes, M.A., Bowcock, A.M., Krueger, J.G., 2007. Pathogenesis and therapy of psoriasis. *Nature* 445, 866–873.
- Manzo, S., 2004. Sea urchin embryotoxicity test: proposal for a simplified bioassay. *Ecotoxicol. Environ.* 57, 123–128.
- Millero, F.J., Woosley, R., 2009. The hydrolysis of Al(III) in NaCl solutions—a model for Fe (III). *Environ. Sci. Technol.* 43, 1818–1823.
- Nedoszytko, B., Sokolowska-Wojdylo, M., Ruckemann-Dziurdzinska, K., Roszkiewicz, J., Nowicki, R.J., 2014. Chemokines and cytokines network in the pathogenesis of the inflammatory skin diseases: atopic dermatitis, psoriasis and skin mastocytosis. *Postepy. Dermatol. Alergol.* 31, 84–91.
- Nomura, I., Gao, B., Boguniewicz, M., Darst, M.A., Travers, J.B., Leung, D.Y., 2003. Distinct patterns of gene expression in the skin lesions of atopic dermatitis and psoriasis: a gene microarray analysis. *J. Allergy Clin. Immunol.* 112, 1195–1202.
- Nurnberg, W., Haas, N., Schadendorf, D., Czarnetzki, B.M., 1995. Interleukin-6 expression in the skin of patients with lupus erythematosus. *Exp. Dermatol.* 4, 52–57.
- Orfanos, C.E., Zouboulis, C.C., Almond-Roesler, B., Geilen, C.C., 1997. Current use and future potential role of retinoids in dermatology. *Drugs* 53, 358–388.
- Oris, J.T., Giesy, J.P.J., 1986. Photoinduced toxicity of anthracene to juvenile bluegill sunfish (*Lepomis macrochirus Rafinesque*): photoperiod effects and predictive hazard evaluation. *Environ. Toxicol. Chem.* 5, 761–768.
- Papakonstantinou, E., Aletras, A.J., Glass, E., Tsogas, P., Dionysopoulos, A., Adjaye, J., Fimmel, S., Gouvousis, P., Herwig, R., Lehrach, H., Zouboulis, C.C., Karakiulakis, G., 2005. Matrix metalloproteinases of epithelial origin in facial sebum of patients with acne and their regulation by isotretinoin. *J. Invest. Dermatol.* 125, 673–684.
- Penagos, H.G., 2002. Contact dermatitis caused by pesticides among banana plantation workers in Panama. *Int. J. Occup. Environ. Health* 8, 14–18.
- Pidwirny, M., 2016. In: Pidwirny, M. (Ed.), *Earth-Sun Relationships and Insolation. Fundamentals of Physical Geography*.
- Ratzinger, G., Stoitzner, P., Ebner, S., Lutz, M.B., Layton, G.T., Rainer, C., Senior, R.M., Shipley, J.M., Fritsch, P., Schuler, G., Romani, N., 2002. Matrix metalloproteinases 9 and 2 are necessary for the migration of Langerhans cells and dermal dendritic cells from human and murine skin. *J. Immunol.* 168, 4361–4371.
- Sawicki, G., Marcoux, Y., Sarkhosh, K., Tredget, E.E., Ghahary, A., 2005. Interaction of keratinocytes and fibroblasts modulates the expression of matrix metalloproteinases-2 and -9 and their inhibitors. *Mol. Cell. Biochem.* 269, 209–216.
- Schneider, C.A., Rasband, W.S., Eliceiri, K.W., 2012. NIH image to imageJ: 25 years of image analysis. *Nat. Methods* 9, 671–675.
- Segre, J.A., 2006. Epidermal barrier formation and recovery in skin disorders. *J. Clin. Invest.* 116, 1150–1158.
- Settivari, R.S., Gehen, S.C., Amado, R.A., Visconti, N.R., Boverhof, D.R., Carney, E.W., 2015. Application of the KeratinoSens assay for assessing the skin sensitization potential of agrochemical active ingredients and formulations. *Regul. Toxicol. Pharmacol.* 72, 350–360.
- Turksen, K., Kupper, T., Degenstein, L., Williams, I., Fuchs, E., 1992. Interleukin 6: insights to its function in skin by overexpression in transgenic mice. *Proc. Natl. Acad. Sci. U. S. A.* 89, 5068–5072.
- UNEP, 2010. *United Nations Environment Programme Annual Report*.
- UNEP, 2012. *United Nations Environment Programme Annual Report*.
- Urban, C., Anadkat, M.J., 2013. A review of cutaneous toxicities from targeted therapies in the treatment of colorectal cancers. *J. Gastrointest. Oncol.* 4, 319–327.
- USDHHS, 1993. *Hazardous Substances Data Bank. National Toxicology Information Program*, Bethesda, MD.
- USEPA, 2006. In: Agency U.S.E.P. (Ed.), *DCNA (Dicloran) Reregistration Eligibility Decision (RED) Fact Sheet*.
- van de Merwe, J.P., Leusch, F.D., 2015. A sensitive and high throughput bacterial luminescence assay for assessing aquatic toxicity—the BLT-screen. *Environ. Sci.: Processes Impacts* 17, 947–955.
- Vebrosky, E.N., Saranjampour, P., Crosby, D.G., Armbrust, K.L., 2018. Photodegradation of dicloran in freshwater and seawater. *J. Agric. Food Chem.* 66, 2654–2659.
- Visse, R., Nagase, H., 2003. Matrix metalloproteinases and tissue inhibitors of metalloproteinases: structure, function, and biochemistry. *Circ. Res.* 92, 827–839.
- Wang, X.P., Schunck, M., Kallen, K.J., Neumann, C., Trautwein, C., Rose-John, S., Proksch, E., 2004. The interleukin-6 cytokine system regulates epidermal permeability barrier homeostasis. *J. Invest. Dermatol.* 123, 124–131.
- Wikramanayake, T.C., Stojadinovic, O., Tomic-Canic, M., 2014. Epidermal differentiation in barrier maintenance and wound healing. *Adv. Wound Care* 3, 272–280.
- Wilgus, T.A., Ross, M.S., Parrett, M.L., Oberyshyn, T.M., 2000. Topical application of a selective cyclooxygenase inhibitor suppresses UVB mediated cutaneous inflammation. *Prostaglandins Other Lipid Mediat.* 62, 367–384.
- Wood, L.C., Jackson, S.M., Elias, P.M., Grunfeld, C., Feingold, K.R., 1992. Cutaneous barrier perturbation stimulates cytokine production in the epidermis of mice. *J. Clin. Invest.* 90, 482–487.
- Wu, K.K., 1996. Cyclooxygenase 2 induction: molecular mechanism and pathophysiologic roles. *J. Lab. Clin. Med.* 128, 242–245.
- Xu, W., Jia, S., Xie, P., Zhong, A., Galiano, R.D., Mustoe, T.A., Hong, S.J., 2014. The expression of proinflammatory genes in epidermal keratinocytes is regulated by hydration status. *J. Invest. Dermatol.* 134, 1044–1055.
- Xu, W., Hong, S.J., Zeitchek, M., Cooper, G., Jia, S., Xie, P., Qureshi, H.A., Zhong, A., Porterfield, M.D., Galiano, R.D., Surmeier, D.J., Mustoe, T.A., 2015a. Hydration status regulates sodium flux and inflammatory pathways through epithelial sodium channel (ENaC) in the skin. *J. Invest. Dermatol.* 135, 796–806.
- Xu, W., Hong, S.J., Zhong, A., Xie, P., Jia, S., Xie, Z., Zeitchek, M., Niknam-Bienia, S., Zhao, J., Porterfield, D.M., Surmeier, D.J., Leung, K.P., Galiano, R.D., Mustoe, T.A., 2015b. Sodium channel Nax is a regulator in epithelial sodium homeostasis. *Sci. Transl. Med.* 7, 312ra177.
- Xu, W., Vebrosky, E.N., Richards, M.L., Armbrust, K.L., 2018. Evaluation of dicloran phototoxicity using primary cardiomyocyte culture from *Crassostrea virginica*. *Sci. Total Environ.* 628–629, 1–10.
- Zhong, A., Xu, W., Zhao, J., Xie, P., Jia, S., Sun, J., Galiano, R.D., Mustoe, T.A., Hong, S.J., 2016. S100A8 and S100A9 are induced by decreased hydration in the epidermis and promote fibroblast activation and fibrosis in the dermis. *Am. J. Pathol.* 186, 109–122.